

## **1-D Assessment of Formation Pressure from Transit Time and Shale Diagenesis of an Onshore Field in Niger Delta**

<sup>1</sup>Aigba, Paul I., <sup>2</sup>Nwankwo, Cyril N. and <sup>2</sup>Ekine, Anthony S.

<sup>1</sup>Department of Physics, Michael Okpara University of Agriculture, Umudike, Abia State, Nigeria

<sup>2</sup>Department of Physics, University of Port Harcourt, Port Harcourt, Nigeria

---

**Abstract:** Modeling formation pressures as an input by the engineers into drilling programs come in different styles and reliability. Kicks, loss of circulation, blowouts and even loss of lives are some of the major tragedies associated with poor modeling. The use of 1D has proved to be a sufficient tool; however, it has fallen short of modeling inflation in formation pressure alongside other pressures. The integration of 1D and clay diagenesis to infer formation pressure is robust. Gamma ray logs were loaded into the log panel for correlation, normal compaction was generated from sonic log while overburden stress (OBS) was estimated from density log. Transit time from sonic was used in obtaining Vertical Effective Stress (VES) by applying an exponent and deducting VES from the OBS to obtain formation pressure (FP). Percentage of Illite/Smectite + Illite (ILLISM) transformation and Kaolinite + Dickite + Halloysite transformation to illite were obtained from clay minerals analysed by X-Ray Diffraction (XRD). These percentages were then tied to formation pressures from the 1D assessment. In Well A, peak geopressures of 5549.12psi and 7873.07psi at 8306.50ft and 11405ft respectively dropped to 6831.92psi at 11566ft. 29% weight of ILLISM recorded at 8090ft, slightly deeper than 8027ft yielded 4407.85psi; 32% ILLISM was present at 8330ft close in depth to 8306ft of 5549.12psi. Depth of 11405ft with formation pressure 873.07psi was 250ft above 11630ft which recorded 25% ILLISM. Well E yielded high overpressures with 6077.89psi and 8085.33psi at the depths of 8259.87ft and 10867.63ft respectively. Mild high formation pressure of 5853.26psi rose steadily at 8819.42ft. Depths of high illite/smectite mix in Well A tied well with its mildly high formation pressure depths. Well E is of high formation pressure.

**Keywords:** Formation pressure, transit time, clay diagenesis, illite/smectite, kaolinite + Dickite + Halloysite,

---

### **I. Introduction**

The rate of dewatering compliments that of sedimentation for normal compaction or hydrostatic pressure to be generated (Sayer, 2006). Consequent upon deposition in a marine atmosphere, sediments exhibit a high porosity and permeability because they are unconsolidated. This results in the communication of pressure of formation water with the surface, and the weight of the solid phase is borne at the matrix contacts without affecting the fluid pressure (Bourgoyne et al., 1986). There is therefore, the need to have a comprehensive study on the diverse causes of formation pressure in the Niger Delta Basin.

The hydrostatic pressure gradient is bounded by 0.43psi/ft on the minima and 0.49psi/ft on the maxima. Furthermore, top of overpressure is marked by mild overpressure which ranges from 0.50-0.69psi/ft while hard overpressure is  $\geq 0.70$ psi/ft. Equilibrium shifts from the hydrostatic pressure owing to excess rate of sedimentation over dewatering process for disequilibrium compaction to occur. In this case, the pressure generated in the subsurface is as a result of seal compartmentalization due to the shale lithology. Here, porosity is driven by the effective stress because of overburden stress of the load carried by the subsurface and permeability experiences a set-back. The formation pressure resulting from the above process is simply of mechanical compaction. However, as the depth of burial increases (>2000 to 3000m), compaction becomes a chemical process under an influence of temperature at window range of 70-100<sup>0</sup>C rather than the former (Fig.1). Conditions governing mechanical compaction vary from that of chemical compaction which is controlled by mineralogy and temperature. Results from compaction modeling are functions of either of the two (Bjørlykke, 1998). The vertical effective stress derived from transit time of sonic log and integrated with clay diagenesis and temperature is a holistic approach to evaluating formation pressure.

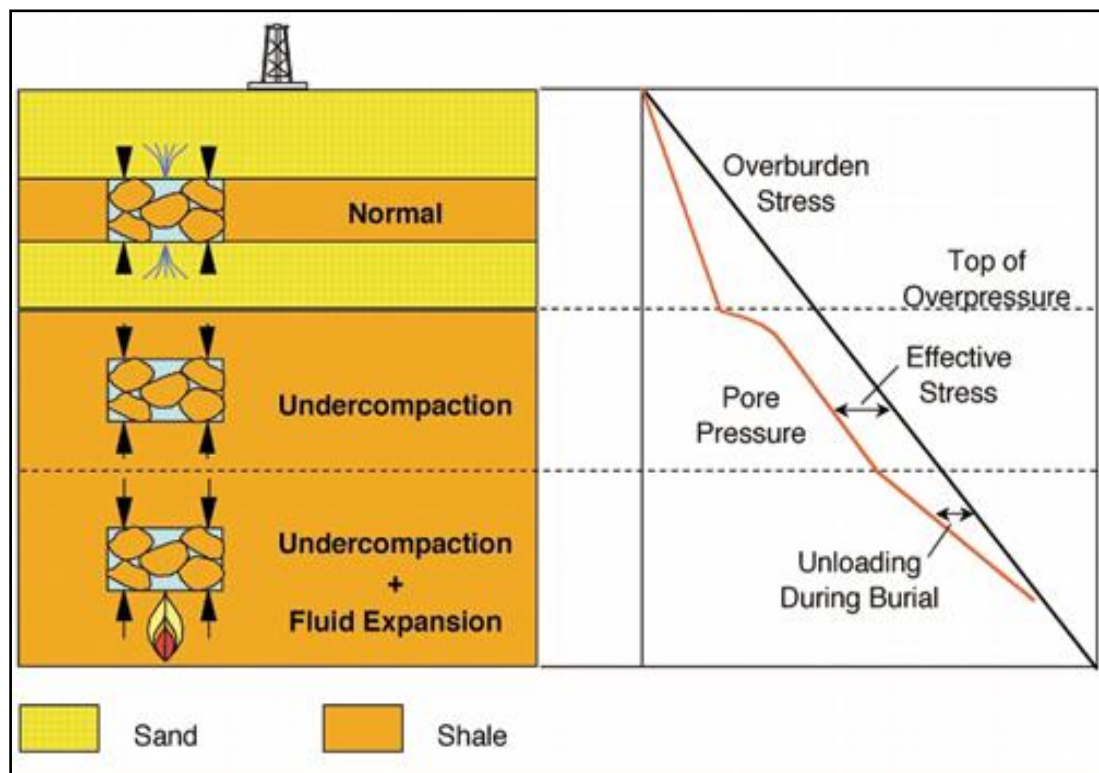


**Fig. 1:** Effect of vertical effective stress on different subsurface conditions (After Bowers, 2002).

Marine shale rich in smectite of tertiary North Sea, are of very low permeability. In such shale masses, normal compaction to observed disequilibrium compaction coupled with related overpressure can take place at slightly less than 1 km burial depth. Nevertheless, chemical transformation of smectite can begin albeit such shallowness, and it is expected that a mineral change to illite and likely chlorite. Marine shale exhibits this universally (Bjørlykke, 1998). Bound water in the smectite layers is released when the temperature reaches this critical temperature, and this results in a porosity decrease.

Alam, et al., (2009) deduced that the slow reduction in the concentration of illite-smectite from older to younger formation in a blended rock is a pointer to the occurrence of diagenesis in such trend. All rocks that are expandable are said to be blended clays. A decreasing concentration of clay mineral in older rock is an indication of another form of diagenesis that involves dissolution and precipitation from younger to older rocks. The latter process occurs in sediments that are deeper (>2-3 km, 70-100°C); are compaction-controlled which rely on temperature and feeble effective stress variation. Total pore water flux depends on rate of compaction rather than pore pressure gradient and permeability.

Ichara and Avbovbo (1985) submitted that only undercompaction is not responsible for the observed geopressures in some parts of Niger Delta but fluid expansion mechanisms comprising offfluid charging, clay diagenesis, and hydrocarbon maturation also immensely contribute to overpressure especially in deep prospects. There appears the existence of connection between high overpressures and compaction disequilibrium, thermal (fluid) expansion mechanisms, shale diagenesis and in particular hydrocarbon generation in the Niger Delta basin (Nwaufaet al., 2006).

The stratigraphy of the Niger Delta is clearly defined by three portions terminating in Recent from Eocene ages (Fig.2). The corresponding topmost Recent Benin Formation is predominantly a deposit of alluvial and upper coastal plain sands of thickness of up to 2km (Avbovbo, 1978). Below this sand and sandstone is an underlying Agbada Formation of shale and sandstone intercalation of 3.7km thickness. It is a major hydrocarbon-bearing formation. The third and deepest underlying Akata Formation is about 6.5km of delta prone clays. Shales of the Akata Formation are overpressure and constitute a world-class source rock. Deepwater sedimentary sand laid down by a turbidite current is equally found to be present in this formation.

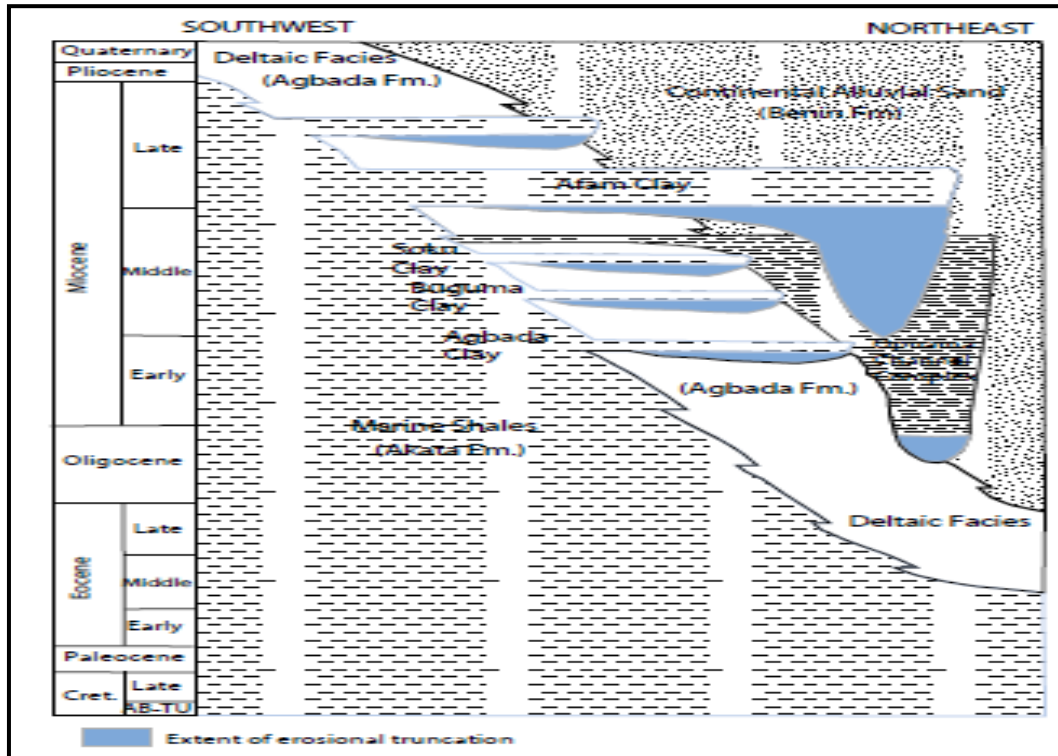


Fig. 2: Stratigraphic column showing the three formations of the Niger Delta (Modified from Shannon and Naylor 1989; Doust and Omatsola, 1990)

**Study area location**

The two wells used for this study are located in Greater Ughelli depobelt onshore Niger Delta (Fig. 3). Locations of Well A and Well E are defined by (X: 482666.64, Y: 153716.81) and the (X: 475373.5, Y: 160069.6) respectively. All coordinates were taken in feet as the wells are about 2km apart in both Easting and Northing.

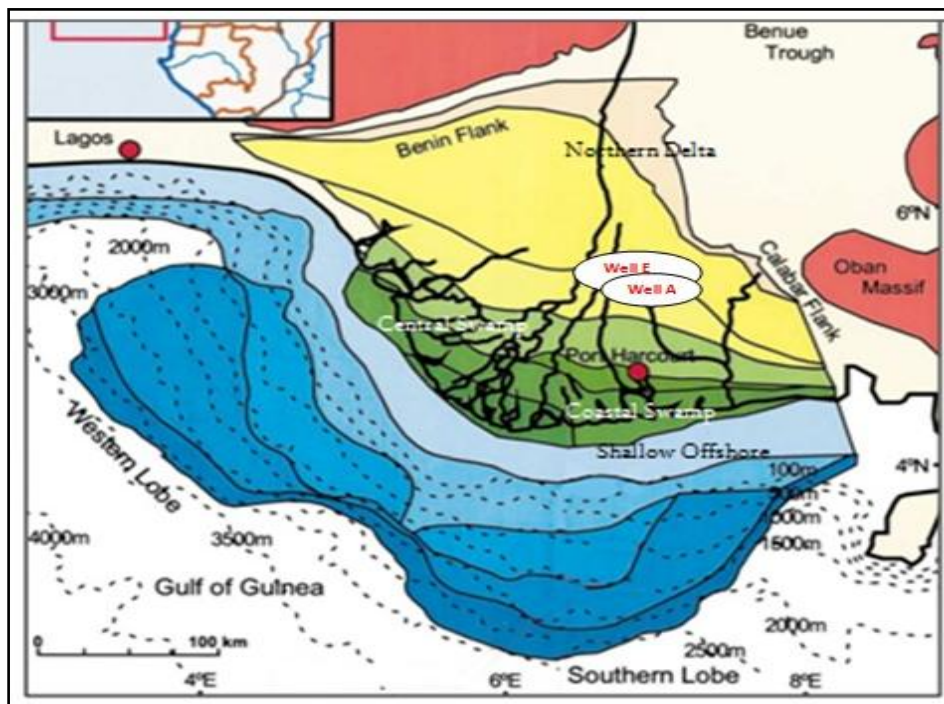


Fig. 3: Map of the Niger Delta showing its different depobelts and sample wells. Wells A and E are in the same field in Greater Ughelli depobelt (Modified from Doust and Omatsola, 1990).

## II. Materials and Methods

The data available for this study include drilling log of Repeat Formation Tester (RFT) that gives the measured formation pressures in sand of the wells; logs of Gamma ray, Density and Sonic which measures the transit time in  $\mu\text{s}/\text{ft}$  used for this study; Checkshot was also available for time-depth conversion. Core samples Clay Minerals data from X-ray Diffraction (XRD) was also obtained from Shell Petroleum Development Company (SPDC, Table 1).

**Table 1:** Results of clay minerals of well A core samples from X-Ray Diffraction as provided by Shell Petroleum Development Company (SPDC).

DEPTH (ft).	K+D+H (% wt)	CHLORITE (% wt)	TOTAL NE CLAYS (% wt)	ILLITE/ILLITE+S MECTITE(MONT) (% wt)	SEPIOLITE+P ALYGORSKITE (% wt)	TOTAL EXP CLAYS (% wt)	MICA(MUSCO) (% wt)
6890	37	33	70	21	0	21	7
7190	38	28	66	16	10	26	8
7490	36	29	65	12	13	25	10
7670	33	18	51	29	20	49	-
7850	26	25	51	12	26	38	11
8090	11	20	31	29	28	57	11
8330	12	13	25	32	37	69	6
8570	1	28	29	22	37	59	12
9230	5	10	15	5	71	76	9
9650	1	20	21	33	33	66	11
9950	0	31	31	54	15	69	-
10610	0	20	20	0	80	80	-
11630	0	18	18	25	57	82	-
12170	0	17	17	49	34	83	-

The XRD results of various clay minerals constituent in the core samples of well A as shown in Table 1 were statistically presented in Figures 4 and 5 and tied to 1D modeled formation pressure (figs. 7 and Table 2).

Imported logs of various wells were correlated using the Gamma ray which delineated the two common lithologies of shale and sand. Normal compaction trend (NCT) was generated using the sonic transit time. The NCT in time domain decreased with depth following the earth model. This is an ideal situation that commemorates the fastness of the sonic (shorter time taken for the signal to transit a more compacted layer than the immediate previous). The time measured in shale along the NCT is the normal time ( $t_{\text{normal}}$ ) while the time traced out by the slowness of the transit time is the observed time ( $t_{\text{observed}}$ ). The density log was used to generate the overburden stress of the formation at different depths:

$$S(h) = g \int_0^h \rho_{\text{bulk}}(z) dz \tag{1}$$

where  $S$  is the overburden stress, an addition of the matrix stress and the pore fluid stress,  $g$  is gravity,  $\rho_{\text{bulk}}$  is the density of bulk formation that depends on depth ( $z$ ) of formation.

The fluid formation pressure (F.P) is derived from the expression of Eaton given as

$$\text{F.P.} = S - \sigma \tag{2}$$

where  $\sigma$  is vertical effective stress of layer which is given as

$$\sigma = \sigma_N \left( \frac{t_{\text{norm}}}{t_{\text{obs}}} \right)^n \tag{3}$$

where  $\sigma_N$  is normal vertical effective stress,  $t_{\text{norm}}$  is the transit time as traced out by the NCT while  $t_{\text{obs}}$  is the observed transit time and  $n$  is the Eaton's exponent. In both cases  $n$  value of 5.5 was used as 3 failed to model the RFT (Tables 2 and 3; Figs. 6 and 8).

## III. Results

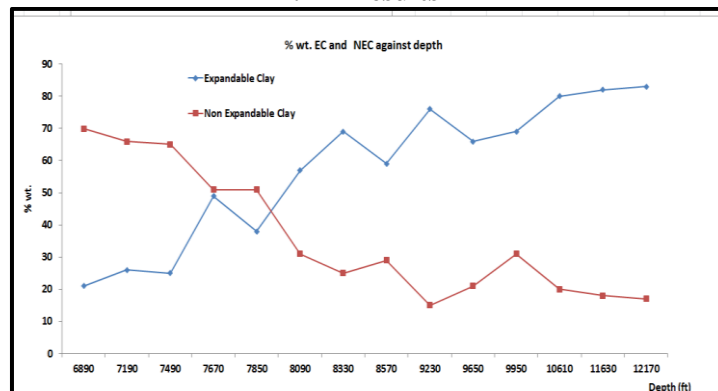


**Fig.4:** Graph of % Clay type against Depth for well A

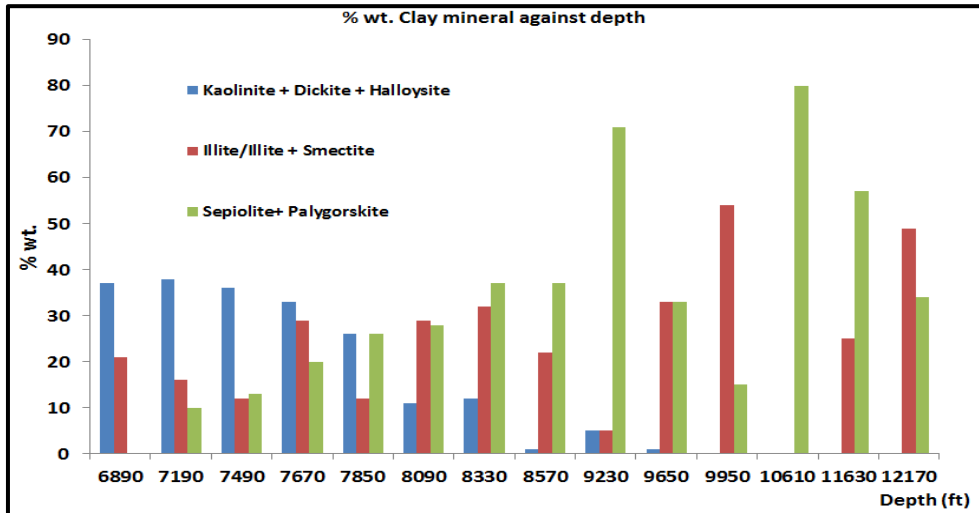


Fig.5: Graph % wt. ILLISM/ SEPA/KDH against Depth (ft) for Well A

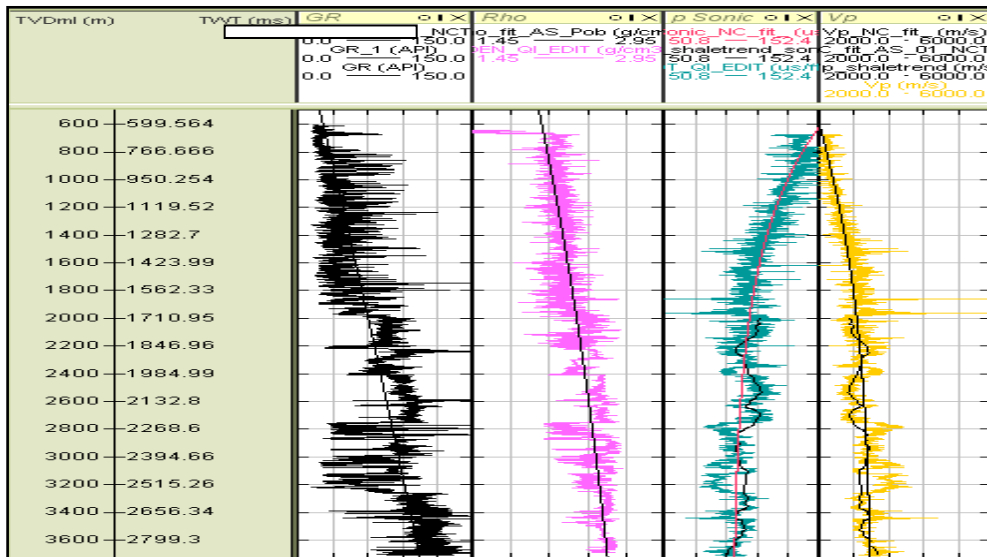


Fig.6: The key logs for Well A

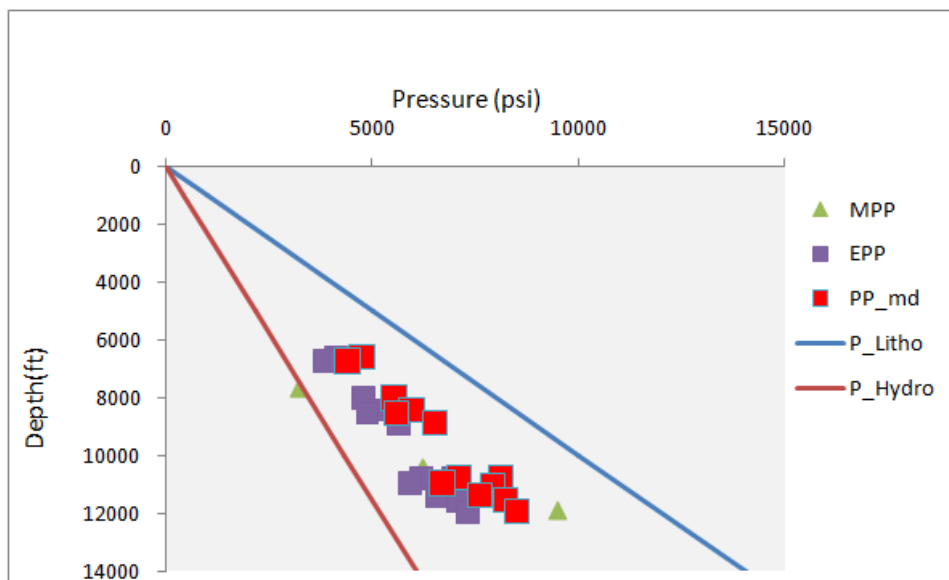
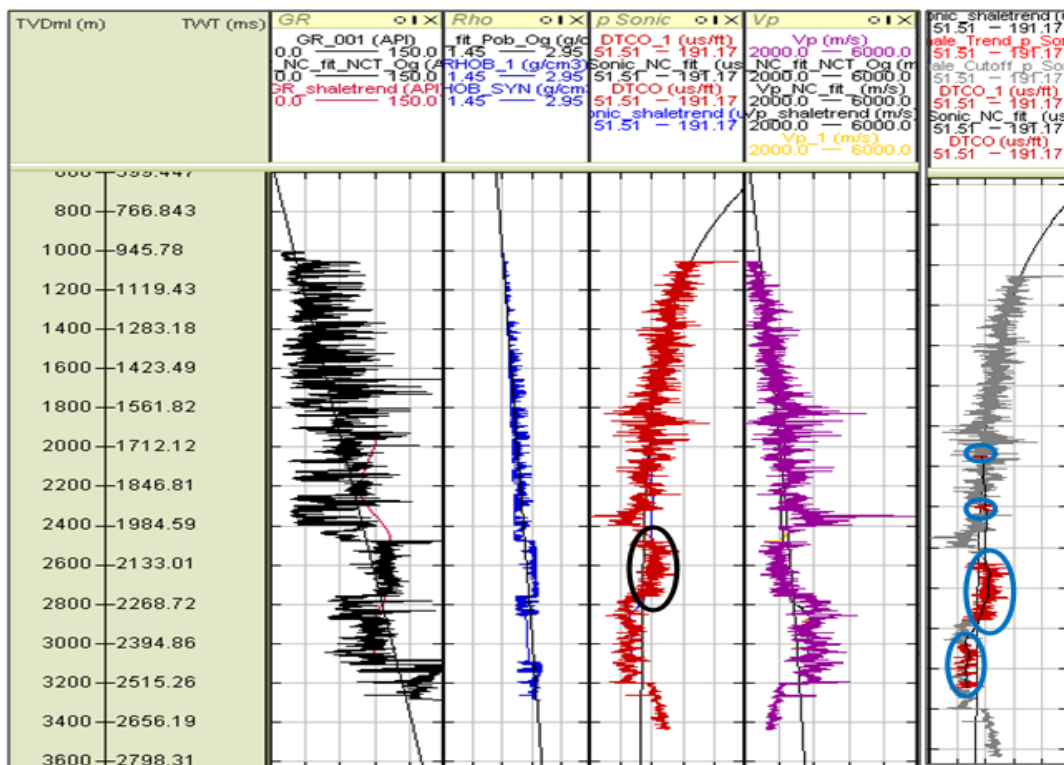


Fig. 7: Graph of Pressure Depth for Well A

**Table 2:** The modeled formation pressure of well A using sonic transit time.

TVD(m)	TVD(ft)	OBS(psi)	tobs	tnorm	PP(psi)	VES(psi)	PP_grad(psi/ft)
865.70	2856.81	2538.18	141.98	138.00	1431.63	1106.54	0.50
903.60	2981.88	2648.65	143.28	136.77	1574.12	1074.53	0.53
928.83	3065.14	2775.29	143.28	135.47	1730.44	1044.85	0.56
1076.04	3550.93	3228.19	132.86	130.26	1713.71	1514.48	0.48
1167.15	3851.60	3550.31	134.16	125.05	2193.23	1357.08	0.57
1204.80	3975.84	3664.36	131.56	122.02	2257.89	1406.47	0.57
1735.00	5726.46	5519.32	119.01	112.02	3201.19	2318.13	0.56
1913.37	6314.12	6029.53	122.44	109.42	4070.28	1959.25	0.64
2004.86	6616.04	6489.02	112.72	105.51	3808.52	2117.72	0.56
2046.80	6754.44	6624.46	112.72	105.51	3878.04	2139.58	0.56
2432.67	8027.81	8148.64	110.32	101.90	4907.85	2587.70	0.62
2517.12	8306.50	8502.94	113.76	101.60	5549.12	2248.11	0.68
2701.10	8913.63	9123.36	114.02	100.30	6016.53	2092.53	0.67
2740.15	9042.50	9607.43	105.51	97.69	5732.51	4404.19	0.67
3281.81	10830.00	11597.50	104.21	97.69	6599.53	3664.77	0.59
3330.24	10989.80	11578.00	101.60	97.69	6994.50	3454.00	0.53
3363.80	11100.50	11790.70	106.81	97.69	7379.34	3225.86	0.64
3456.07	11405.00	12212.50	109.42	97.69	7873.07	3043.93	0.68
3504.85	11566.00	12484.80	104.21	97.69	6831.92	5652.84	0.59



**Fig. 8:** Composite log of Well E showing shale trend plots in circled sky-blue colour in the extreme right track.

Well E has a prominent transit time increase in shale as indicated by the black-circled portion on the third track (Fig. 8). The result of formation pressure (fig.9) shows a better prediction with n=5.5 for PP\_md than n=3 PPP.

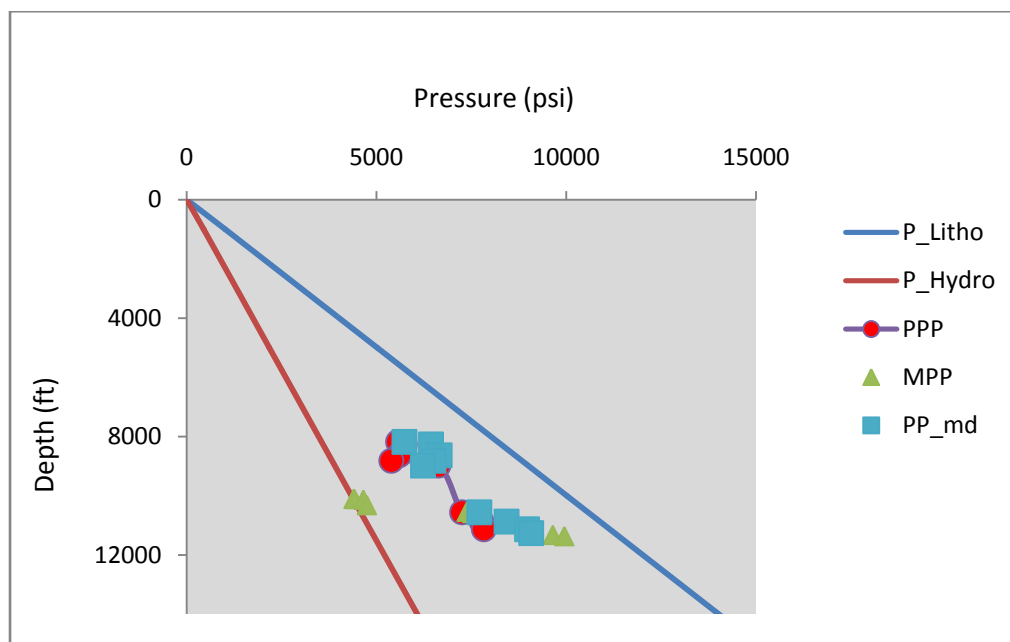


**Fig. 9:** Formation pressure depth analysis of well E

**Table 3:** The modeled formation pressure of Well E using sonic transit time

TVD(ft)	TVD(m)	OBS(psi)	tobs	tnorm	PP(psi)	VES(psi)	PP_grad(psi/ft)
1365.09	413.66	3927.62	125.58	119.72	2419.08	1508.54	0.54
1751.95	530.89	5288.08	115.47	106.72	3492.07	1796.01	0.60
1936.75	586.89	5740.59	119.11	105.10	4254.31	1486.29	0.67
2184.57	661.99	6351.20	108.06	100.23	4225.51	2125.69	0.59
8179.94	2478.77	7402.73	116.66	100.23	5371.47	2031.25	0.66
8259.87	2502.99	7553.57	126.16	100.23	6077.89	1475.68	0.74
8632.90	2616.03	8007.53	121.61	98.60	5922.44	2085.10	0.69
8819.42	2672.55	8158.37	117.38	98.60	5853.26	2305.11	0.66
8979.30	2721.00	8158.37	111.90	96.98	6051.59	2106.78	0.67
10558.58	3199.57	9820.51	114.35	96.98	7526.08	2294.42	0.71
10867.63	3293.22	10122.18	117.71	95.36	8085.33	2036.86	0.74

#### IV. Discussion of Results

Table 1 shows a breakdown of the clay mineral contents of the core of Well A. The absolute values of the various constituents of Expandable clay (comprising of illite/smectite + illite and Sepiolite + Palygorskite), Non expandable clay (comprising of chlorite and kaolinite + Dickite + Halloysite) and Mica (muscovite) were observed to be in existence.

The results of various clay minerals of the core of Well A were plotted in percentage weight against depths of burial (age). Figure 6 brings to fore the statistical analysis of the activities of these minerals at various depths. A graphical analysis of the Expandable clay and Non expandable clay showed that the shallow depths favoured higher concentrations of the Non expandable clay (NEC) and lower concentrations of Expandable clay (EC) (Fig.4). There was a characteristic downward trend as exhibited by NEC while EC enjoyed a notch up in concentration on the aggregate. A plateau of 51% NEC occurred between 7670ft and 7850ft and subsequently continued its relative downward trend. At 9650ft, EC continued with its steady rise.

Figure 5 showed that Kaolinite + Dickite + Halloysite (KDH) was active in the shallow depths and continued its depreciation until it finally disappeared completely at 9950ft and below. The illite/smectite + illite mix has an undefined trend in distribution before 11630ft; however, beyond this depth, an increasing trend unfolded. The change of the nature of interstratifications of illite and smectite layer takes place from random to an ordered fashion (Perry and Hower, 1970).

The existence of Sepiolite + Palygorskite mix can be divided into three tranches; (i) a steady increase from 10% at 7190ft to a peak of 71% at 9230ft; (ii) a steady decline from this peak to 15% at 9950ft; and (iii) its sole existence of the highest value of 80% at 10610ft and steady decline up to the total depth of the well at 12170ft. It rather takes tough conditions for SEPA to transform into smectite. Mumpton and Roy (1956) hydrothermally accomplished the transformation of SEPA to smectite at a temperature of 200°C and a water pressure of 20,000psi (Ultra High Pressure/High Temperature well, Courtesy of Halliburton, 2012 in Shadravan and Amani, 2012). Solution and re-precipitation seems to be a common process for the transformation of Palygorskite and Sepiolite to smectite. The partial breakdown and rearrangement of the former occurs simultaneously with precipitation (Golden, et al., 1985).

The third track on the log panel is the sonic plot (Fig. 6) showing the red line (normal transit time,  $t_{normal}$ ) and some slow transit time ( $t_{obs}$ ) points. After imposing the Eaton's model of exponent of 3 to obtain EPP and exponent of 5.5 PP\_md, the trend of the MPP (RFT) was better modeled by the EPP (Fig. 7). Sonic transit time experienced slowness at the corresponding depths of red-circled time, thereby showing increase in formation pressures though mild at such points (Table 2). Peak geopressures of 5549.12psi and 7873.07psi played out at both 8306.50ft and 11405ft respectively and dropped to 6831.92psi at 11566ft. 29% weight of illite/smectite + illite (ILLSM) was recorded at 8090ft (Table 1) close to 8027ft that yielded 4907.85psi (Table 2); 32% ILLISM was present at 8330ft close to 8306ft of 5549.12psi. Finally, 11405ft of 7873.07psi was less than 250ft above 11630ft which recorded 25% ILLISM.

Increase in transit time signifying slowness in sonic were recorded by the red-circled times Table 3) for Well E. Such, eventually yielded high formation pressures of 6077.89psi and 8085.33psi at the depths of 8259.87ft and 10867.63ft respectively. Formation pressure of 5371.47psi rose steadily at 8819.42ft. There were no clay minerals data to correlate formation pressure of this well.

## V. Conclusion

The total disappearance of KDH in older rocks is in agreement with its trend in similar sediments worldwide. Smectite/ illite mix was sporadically higher than SEPA at only four (4) points while the latter was predominant at many points. The reduction in quantity of ILLISM in clay minerals data corresponded well with points of relatively high formation pressure in Well A. However, it may be said that clay diagenesis remotely constituted to its formation pressure. Well E has formation pressures that translate to high overpressures at some depths. The slowness in transit time like velocity reversal in shale was able to deduce formation pressure of both wells. The overpressures in this field increased in the North West direction.

## Acknowledgement

The authors are indeed grateful to Shell Petroleum Development Company (SPDC) for providing the data used for this research work. We are also indebted to Ikon science.

## References

- [1]. Alam, M., A.K.M., Xie, S. and Chowdbury, S.Q., (2009): Clay Mineralogy and Diagenesis of Shale: A case study from Mio-Pliocene Tipam and Dupi Tilashales of Bandarban Anticline Hill District, Bangladesh. ISSN 1812-5654 Asian Network for Scientific Information. Journal of Applied Science 9(15): 2770-2777.
- [2]. Avbovbo, A. A., (1978): Tertiary lithostratigraphy of Niger Delta: AAPG Bulletin, v. 62, p. 295-300.
- [3]. Bjørlykke, K., (1998): Clay mineral diagenesis in sedimentary basins a key to the prediction of rock properties. Examples from the North Sea Basin
- [4]. Bourgoyne Jr., A.T., Chenevert, M.E., Millheim, K. and Young Jr. F.S. (1986): Applied Drilling Engineering Richardson: SPE Textbook Series.
- [5]. Bowers, G.L. (2002): Detecting high overpressure, Applied Mechanics Technologies, Houston, Texas, U.S. The leading edge, Feb. 2002, pp 174-177.
- [6]. Doust, H., and Omatsola, E., (1990): Niger Delta, in, Edwards, J.D., and Santogrossi, P.A., eds., Divergent/Passive Margin Basins. AAPG Memoir 48: pp. 239-248
- [7]. Evamy, B.D., Haremboure, J., Kamerling, P., Knaap, W.A., Molloy, F.A., and Rowlands, P.H., 1978, Hydrocarbon habitat of Tertiary Niger Delta: AAPG Bulletin, v. 62, p. 277-298.
- [8]. Golden, D. C., Dixon, J. B., Shadfai, H., and Kippenberger, L. A. (1985): Palygorskite and Sepiolite alteration to smectite under alkaline conditions, Soil and Crop Science Department, Texas A&M University College Station, Texas 77843, Clays and Clay Minerals, Vol. 33, No. 1, 1985, p. 44-50
- [9]. Ichara M.J. and Avbovbo A.A. (1985): How to handle abnormal pressures in Nigeria's Niger Delta area, J. Petrol. Technol. 83, 10, 122-124.
- [10]. Mumpton, F. A. and Roy, R. (1956): New data on Sepiolite and attapulgite, Clays and Clay Minerals, Proc. 5th National Conference., Urbana, Illinois, 1955, Ada Swineford, ed., National Academy of Science., Natl. Res. Council. Publ. 566, p. 136-143.

- [11]. Nwaufa W.A., Horsfall D.E. and Ojo C.A. (2006):Advances in deep drilling in the Niger delta, 1970-2000: Nigerian Agip Oil Company (NAOC) Experience, Nigerian Association Petroleum Explorers' Conference, Abuja Nigeria, August 2006, pp. 5-14.
- [12]. Perry, E.A. and Hower, J., (1970): Burial diagenesis in Gulf Coast sediments, Clays, Clay Minerals, 18: pg. 165-177.
- [13]. Sayers, C.M.(2006): An introduction to velocity-based pore-pressure estimation Schlumberger Data and Consulting Services Houston, USA. The leading edge Dec. 2006, pp.1496-1500.
- [14]. Shadravan A. and Amani M. (2012):HPHT 101-What Petroleum Engineers and Geoscientists Should Know About High Pressure High Temperature Wells EnvironmentEnergy Science and Technology,Vol.4, No. 2, 2012, pp. 36-60DOI:10.3968/j.est.1923847920120402.635
- [15]. Shannon, P. M., and Naylor N., 1989, Petroleum Basin Studies: London,Graham and Trotman Limited, p 153-169.
- [16]. Tuttle, M.L.W., Charpentier, R.R. and Brownfield, M.E. (1999):The Niger Delta Petroleum System: Niger Delta Province, Nigeria, Cameroon, and Equatorial Guinea, Africa, Tertiary Niger Delta (Akata-Agbada) Petroleum System (No. 701901), Niger Delta Province, Nigeria, Cameroon, and Equatorial Guinea, Africa . U.S. Geological Survey, Department of the Interior.